



**HAL**  
open science

## Study of uniaxial deformation behavior of 50 nm-thick thin film of gold single crystal using in situ X-ray pole figure measurements

J. Drieu La Rochelle, P. Godard, C. Mocuta, D. Thiaudière, J. Nicolai, M.F. Beaufort, M. Drouet, P.O. Renault

### ► To cite this version:

J. Drieu La Rochelle, P. Godard, C. Mocuta, D. Thiaudière, J. Nicolai, et al.. Study of uniaxial deformation behavior of 50 nm-thick thin film of gold single crystal using in situ X-ray pole figure measurements. *Surface and Coatings Technology*, 2019, 377, pp.124878 -. 10.1016/j.surfcoat.2019.06.103 . hal-03488209

**HAL Id: hal-03488209**

**<https://hal.science/hal-03488209>**

Submitted on 20 Jul 2022

**HAL** is a multi-disciplinary open access archive for the deposit and dissemination of scientific research documents, whether they are published or not. The documents may come from teaching and research institutions in France or abroad, or from public or private research centers.

L'archive ouverte pluridisciplinaire **HAL**, est destinée au dépôt et à la diffusion de documents scientifiques de niveau recherche, publiés ou non, émanant des établissements d'enseignement et de recherche français ou étrangers, des laboratoires publics ou privés.



Distributed under a Creative Commons Attribution - NonCommercial 4.0 International License

## Study of Uniaxial Deformation Behavior of 50 nm-thick Thin Film of Gold Single Crystal using in situ X-ray Pole Figure Measurements

J. Drieu La Rochelle<sup>1</sup>, P. Godard<sup>1</sup>, C. Mocuta<sup>2</sup>, D. Thiaudière<sup>2</sup>, J. Nicolai<sup>1</sup>, M.F. Beaufort<sup>1</sup>, M. Drouet<sup>1</sup>, P.O. Renault<sup>1\*</sup>

<sup>1</sup> Institut Pprime, CNRS – Université de Poitiers, 86962 Poitiers cedex, France

<sup>2</sup> synchrotron SOLEIL, L'orme des merisiers Saint Aubin, 91192 Gif-sur-Yvette, France

**Abstract:** In this paper, *in situ* measurements of synchrotron x-ray pole figure have been performed during incremental uniaxial deformation test on a single-crystal gold foil. The 50 nm thick Au thin film was elaborated by ion sputtering at 400°C on NaCl single crystal as a template. The resulting film consists of a single-crystal gold foil containing a small density of thin and small {111} growth twins (few nm thick and few tens of nm long) revealed by x-ray pole figure measurement. The as-deposited gold single crystal was then transferred onto flexible polyimide substrates for deformation test. This work focuses on the relative evolution of the diffracting volume related to growth twins during a loading-unloading tensile test. Macroscopic applied deformations and x-ray pole figures were measured in situ during a uniaxial tensile test in the Au [110] direction. X-ray pole figures clearly evidenced the relative evolution of the diffracting volumes related to the (111) and ( $\bar{1}\bar{1}1$ ) twins which exhibit a huge increase of about 450% at a uniaxial applied true strain of about 4%. The concomitant variation of diffracting volumes related to the two other twin variants (namely ( $\bar{1}1\bar{1}$ ) and ( $1\bar{1}1$ ) twins) shows a relatively low decrease of 25%. The results open out onto a true strain-twinning volume hysteresis curve, indicative of the deformation mechanisms of gold thin films that can be interpreted as a twinning-detwinning mechanism.

Corresponding author: pierre.olivier.renault@univ-poitiers.fr

**Keywords:** *In situ* deformation; Synchrotron X-ray diffraction; mechanical twins; mechanical properties; metallic thin films; single-crystal thin films.

## 1. Introduction

Due to the increasing production and commercialization of various kinds of micro- and nano-electro-mechanical systems, the interest on mechanical behavior of metallic thin films and nanowires has gained considerable attention in the past few decades. In this way, metallic thin films on flexible substrates have wide range of applications such as compliant microelectronic devices biosensors. The analyses of mechanical response, the knowledge of the mechanical properties and the identification of mechanical failure of such metallic nano-crystalline materials may help to find solutions for new design.

Deformation twinning is one of the important deformation mechanisms in face-centered cubic (fcc) metals with a low stacking fault energy (SFE) [1, 2]. As nanotwinned films exhibit interesting mechanical properties, a fundamental understanding of the mechanisms of the twin nucleation and twin growth is essential to capture the mechanical behavior of fcc materials. Twinning deformation is known to be responsible of high mechanical properties of some fcc metals [3-8]. In spite of a lot of efforts that have been undertaken to understand how the deformation process is associated with twinning from the 50s [1] up to the present years [8], there are still some needs to precisely quantify this deformation process. Twinning can occur more frequently in nanostructured metals and can play a more important role in plastic deformation than in their microcrystalline bulk counterpart. Experimentally, a strong effect of the crystal size on deformation twinning has been reported [9]. Molecular dynamic simulations have shown that twins are mainly nucleated from free surface in thin films or nanowires [10]. Very recently, Bejaud *et al.* have shown that steps at the surface of metallic thin films are privileged sites for twin nucleation at lower stresses [11]. H.S. Park *et al.* showed the important

effect that surface orientation can have on the deformation mode via slip or twinning in nanowires [10]. Effect of alloying can also have a significant effect on the twin-based plasticity mechanisms as shown by Ye *et al.* [12]. They conducted *in situ* uniaxial compression experiments on single crystalline Mg and Mg–0.2%Ce nano-pillars inside a Transmission Electron Microscope (TEM) and revealed the presence of strong size effects associated with two distinct mechanisms: basal plane sliding and extension twinning in both materials with a dramatic reduction in critical stress for extension twinning between these two materials.

Studies on single crystals are obviously interesting to understand the deformation mechanisms and, more specifically, single-crystalline films have a favorable microstructure for analyzing the scaling behavior of the mechanical properties. It is relatively easy to fabricate few nanometer thick metallic single crystals. During the 1960s and 1970s, a lot of research was carried out on epitaxial growth of metallic thin films evaporated on alkali halide surfaces [13-16]. In their work, Ino and collaborators [13,14] studied the effect of the substrate temperature and vacuum conditions on the preferred orientation of the deposits of different metals. For another example, Matthews and Allison [16] studied the formation of twins of evaporated fcc metals on NaCl. Much more recently, Dehm *et al.* [17] analyzed the density of nanotwins in gold single-crystals 40-160 nm thick. They observed an increase in twin density with decreasing film thickness that was explained by kinematical and thermodynamical arguments. Single-crystal foils may contain growth twins depending on the growth parameters that can affect the mechanical behavior and induce specific deformation processes like those reported in nanocrystalline materials [3-8]. Even twinning in a high SFE material such as Pd [18] or Al [19] has been observed; it is attributed to emission of twinning partials from the grain boundaries because the nanograins are almost dislocation-free. However, the detailed microstructural aspects as the quantitative development of twins in ultrafine structure such as a thin film in the tens of nanometer range are not well understood.

The study of plastic deformation and fracture of single-crystal films of fcc metals started in 1960 with Catlin and Walker [20] who reported that one of the most interesting of their results was the appearance of bands due to mechanical twinning in single-crystal gold films 100-300 nm thick. Matthews [21] reported the role of mechanical twins in the fracture of single fcc crystals such as gold. More recently, Oh *et al.* [22] performed *in situ* TEM straining experiments on Au single crystal of a few tens of nanometer thick deposited on polyimide substrate. They reported a very interesting transition in the mechanisms of plastic deformation at a thickness of about 80 nm. The films thinner than 80 nm deform through the glide of perfect threading dislocations and Shockley partials on {111} planes while films thicker than 80 nm deform through the glide of perfect dislocations. If several mechanisms of plastic deformation dislocation are proposed, an experimental relationship between the applied deformation and the related mechanism is still lacking. Gruber *et al.* [23] have performed an *in situ* synchrotron-based tensile testing technique to study the mechanical behavior of the same gold single-crystal films. Interestingly, they reported a transition of the dominant plastic deformation mechanism from full to partial dislocations in films thinner than 160 nm. However, the thinner films have a higher density of voids that may facilitate the nucleation of these partial dislocations.

The present experimental study focuses on the deformation mechanisms of a gold single-crystal foil studied by x-ray diffraction. The aim was to add quantitative values to the twinning deformation mechanisms *in situ* at relatively small applied strains. The 50 nm thick foil is deposited onto polyimide substrate and submitted to tensile loading-unloading. Indeed metallic film on polymer substrates can be stretched well beyond the fracture strain of their free-standing metal film counterpart [24, 25]. The tensile loading has been performed in the [110] direction of gold up to a true strain of about 4%. The microstructure of gold single crystal and the x-ray pole figures of {111} planes are presented and discussed. Up to a tensile deformation of about 1%, no significant change appears on the *in situ* Au (111) pole figures. The gold foils

remains in the elasto-plastic regime, certainly based on dislocation activity. Then, from tensile deformations from 1% up to 4%, the diffracted intensity of two of the three measured peaks related to {111} twins drastically increases by a value of the order of 450% unlike the intensity of the third peak which only decreases by 25%. In this strain range, the gold foil exhibits a mechanical deformation that is based on the relative increase of the initial twinning volume related to the (111) and ( $\bar{1}\bar{1}1$ ) twins. The true strain- twin volume curves exhibit a hysteresis that could reveal a de-twinning during unloading.

## **2. Experimental**

### **2.1 Sample elaboration and characterization**

The gold thin films with a (001) orientation were prepared by ion beam sputtering on a single crystal of sodium chloride. The NaCl substrates were cleaved along (001) plane just before installation in the vacuum deposition chamber. The NaCl surface is 10 x 10 mm<sup>2</sup>. The cleaving produces a relatively flat and clean surface that is composed of very flat terraces and cleavage steps that can be observed by optical microscopy. When the pressure had been reduced to about 7x10<sup>-5</sup> Pa, the NaCl substrate was raised to a temperature of 400°C for 1 hour. Then the temperature was maintained at 400 ° C to perform the deposit of gold with an Ar<sup>+</sup> ion gun sputtering beam at 1.2 keV and a working pressure of approximately 10<sup>-2</sup> Pa. Growth rate measurement of 0.15 nm/s was performed by determining the film thickness using *ex situ* x-ray reflectometry measurement. Finally, for the in situ synchrotron experiment, a NaCl substrate had been dissolved in water, and the gold thin film that floats on the surface of the water was simply caught at the center of the polyimide substrate. The 50 μm thick polyimide substrate (kapton HN®) has a cruciform shape with arms of 200 mm long and 20 mm wide (see Geandier *et al.* for the details of the cruciform geometry [26]). Interestingly, even if no specific surface treatment nor adhesion layer nor glue is used, the adhesion is rather good. For

example, the gold film is difficult to extract even using a sticky tape; thus the deformations will be considered as fully transmitted through metal-polyimide interface. Metallic thin film on polymers are much easier to handle and can be stretched well beyond the fracture strain of their free-standing counterpart [24, 25].

The in-plane orientation and the epitaxial relationships of the gold film on NaCl were determined via x-ray pole figures on another gold film. The pole figures have been performed on a Seifert diffractometer (3003 PTS-HR) with a four-circle diffractometer equipped with a copper anode (punctual focus) with a 0.5 mm diameter circular collimator. The x-ray diffracted signal was recorded using a point detector with a curved graphite crystal monochromator in front (selecting only  $K\alpha_1$  and  $K\alpha_2$  of Cu lines) and a 3 mm slit. The step widths for scans of  $\phi$  ( $0 \leq \phi \leq 359^\circ$ ) and  $\psi$  ( $0 \leq \psi \leq 80^\circ$ ) were  $\Delta\psi=0.5^\circ$  and  $\Delta\phi=1^\circ$ .

Conventional, High-Resolution TEM and Scanning TEM (STEM) images were carried out using a JEOL 2200 FS (Schottky-FEG, 200 kV). To realize plane view TEM (Fig.5 Top) the samples were immersed in deionized water to dissolve NaCl. Then, the gold film was transferred to a copper grid. Cross-sectional TEM (XTEM) samples were prepared by Focused Ion Beam (FIB) using an FEI-HELIOS dual-beam using the standard lift-out method [27]. Pt was deposited on the top surface of the sample, then thin foil has been extracted using Ga at 30kV. Thin foil has been thinned using Ga at 30kV and finished at 5kV.

## **2.2 Tensile loading and *in situ* pole figure measurements**

We have used the DIFFABS-SOLEIL biaxial tensile tester working in the synchrotron environment for *in situ* diffraction measurements for thin crystalline films mechanical response [26]. The biaxial loading device was installed on the 6 circle diffractometer (kappa geometry) at the DiffAbs beamline of the SOLEIL Synchrotron (Gif-sur-Yvette, France). A pole figure measurement is performed as follows (Fig. 1): two axes of the diffractometer are used to set

the Bragg angle: the detector is positioned (fixed) at the corresponding chosen diffraction angle  $2\theta$  and the incident angle is set (fixed) to half of this value (with the sample normal to surface being in the vertical plane). Then, the x-ray diffracted intensity is recorded while the sample is rotated around its surface normal (azimuth angle  $\phi$ ) and around the incident x-ray beam direction projected on the sample surface, F1 direction (*i.e.* elevation angle  $\psi$ , defined as the angle between the normal to the surface and the vertical scattering plane) (Fig. 1). Thus a pole figure probes the distribution of orientations in the sample of a crystallographic plane family. In this way, the different orientations of the crystal plane under investigation can be brought into Bragg diffraction condition; the diffraction intensity scales with the crystalline volume with that specific orientation. This tensile tester allows measuring x-ray diffraction in reflection mode from  $0^\circ$  up to high elevation angles ( $\psi$ ); there is almost no shadowing edge. Two couples of motors and force sensors are fixed to the device frame. The four motors can be actuated separately in order to keep the studied area at a fixed position in the goniometer. The cruciform substrates were gripped by a cam rotating in a cylindrical fixation. In addition, the in-plane macroscopic strains ( $\epsilon_{11}$  and  $\epsilon_{22}$ ) of the polyimide substrate (opposite surface) were measured by Digital Image Correlation (DIC) [28, 29] at the center of the cruciform shape substrate by using images of about  $6 \times 9 \text{ mm}^2$ . Noteworthy, the applied strain is homogeneous over this area.

The energy of the incoming monochromatic x-ray beam was 9 keV corresponding to a wavelength of  $\lambda = 0.13776 \text{ nm}$  using a double-crystal monochromator. The beamsize was of  $316 \times 271 \text{ }\mu\text{m}^2$  (horizontal and vertical full width at half maximum, FWHM, respectively). A monitor detector was measuring the intensity of the incident x-ray beam during the in situ experiment. A hybrid pixel area detector (XPAD detector, acronym for x-ray Pixel chip with Adaptable Dynamics [30]) was used at a sample detector distance of 621 mm. It contains  $240 \times 560$  pixels, with a pixel size of  $130 \times 130 \text{ }\mu\text{m}^2$ . The *in situ* pole figure measurements have

been performed on the {111} planes of gold with an incident  $\omega$  angle fixed at  $17^\circ$  and the center of the 2D detector fixed at a  $2\theta$  angle of  $34^\circ$ . As the long side of the detector was mounted in the  $2\theta$  direction (see Fig. 1), the geometrical diffraction conditions resulted in a  $2\theta$  angular acceptance determined to be  $6.8^\circ$ , and around  $5.1^\circ$  in the perpendicular direction (Fig. 2); this perpendicular direction mainly corresponds to  $\psi$  in the pole figure. So, in order to have a significant overlap between two sequential  $\psi$  steps, the sample elevation angle ( $\psi$ ) moved by steps  $\Delta\psi$  of  $3^\circ$  from  $\psi=0^\circ$  to  $81^\circ$ . Moreover, the area detector acquired a snapshot every 100 ms during a continuous in-plane rotation of the sample azimuth (denoted as the  $\phi$  angle), rotating at a speed of  $8^\circ \text{ s}^{-1}$  and covering  $210^\circ$  in  $\phi$ . In other words, a diffraction pattern was continuously recorded with a step  $\Delta\phi$  of  $0.8^\circ$ . The  $\psi$  and  $\phi$  ranges have been chosen by exploiting the four-fold symmetry of the Au (001) single-crystal, the two-fold symmetry of the tensile test and the fact that the main interesting poles are situated at  $\psi$  angles of about  $15^\circ$  and  $55^\circ$ . This set-up enables the measurement of a set of pole figures within 29 min. Thanks to a homemade python code, the raw data were re-calculated to usual angular ( $\psi, \phi$ ) space and the resulting datasets are presented as a standard pole figure [31]. In principle, for a quantitative study, the measured intensity of the gold thin film should be corrected for the defocusing and background effects and the volume of diffracting material and absorption. But these corrections are not necessary as the presented results only focus on the relative quantification of the same poles.

The measurements of x-ray pole figure were performed while subjected to a quasi-uniaxial tension deformation state at progressively higher applied load and then unloaded. Indeed, the component  $\epsilon_{22}$  is kept roughly constant around zero while the component  $\epsilon_{11}$  increases up to 4% (see Fig. 3). The loading of the sample was controlled by displacement of the grips in the two perpendicular directions (labelled 1 and 2 in Fig. 1) with a ratio of 1/4 in order to have a

quasi-uniaxial deformation at the center of the cruciform shape substrate. Fig. 3 shows the applied loads increments and the related applied strain increments; at each increment 10 images were taken before and again 10 after collection time for an x-ray pole figure (i.e. 29 minutes later). On the one hand, the true strain at the center of the cruciform remains constant during interrupted loading intervals for the first part of the test (up to approximately 2.5%). This observation makes it possible to design unique experiments for the study of the relaxation of thin films [32]. On the other hand, as emphasized in the inset of Fig.3, from applied strain larger than 2.5%, there is an apparent decrease of the true strain  $\epsilon_{11}$  but it is only because no DIC measurements are performed during x-ray measurements (i.e. 29 minutes). The apparent drop corresponds to a continuous relaxation of the substrate which rises up to about 0.001 for applied true strains in the range 0.035-0.04. Hence, the relaxation of the center of the cruciform substrate is negligible even for the largest applied strains. Noteworthy, the maximum strain of about 4% is measured at the center of the cruciform shape substrate, this corresponds to the elastic domain of polyimide (Kapton ®HN Dupont™). However, the deformations in other part of the sample are much larger than 4% and more specifically in the toe weld regions. So considering the whole sample, the deformation test is over the yield point and this is why the applied strain at the center of the cruciform shape substrate is not going back to zero when the sample is unloaded (see Fig. 3). Once unloaded, the applied true strain  $\epsilon_{11}$  is equal to 1.8%.

### **3. Results and discussion**

#### **3.1 Microstructure of the as-deposited Au single crystal**

The {111} x-ray pole figure shown in Fig. 4 exhibits the four-fold symmetry in {111} poles indicating that the sample is [001] oriented. As reported by many authors [13-17, 20-23] despite the very large lattice mismatch (0.408 nm for gold and 0.564 nm for NaCl), gold grew with a cube-on-cube orientation relationships: Au (001)//NaCl (001) and Au [100]//NaCl [100]. The

selection of a particular texture of the film depends on a number of kinetic and thermodynamic effects. In the 60s, Ino *et al.* [13] studied the effect of temperature on the different texture components of fcc metals, Matthews [15] reported the importance of contaminants. So in view of the experimental deposition parameters, the cube-on-cube growth of Au was well expected. The {111} pole figure also shows other peaks of much smaller intensity at  $\psi$  angles of about  $16^\circ$  and  $78^\circ$ ; these secondary peaks are attributed to {111} twins. Indeed a {111} twinning volume induces peaks at  $15.8^\circ$ ,  $54.7^\circ$  and  $78.9^\circ$ . Due to the four-fold symmetry of gold, four different twins I, II, III and IV as labeled in Fig. 4 are planned giving rise each to 4 secondary peaks: one at  $15.8^\circ$ , one at  $54.7^\circ$  and two at  $78.9^\circ$  (see dashed circle in Fig. 4 for twins I). Obviously, the intensity arising from the twinning volume at  $54.7^\circ$  is completely negligible compared to the intensity of the gold matrix. The fact that the measured twinning peaks are about 3 orders of magnitudes weaker than the epitaxial peaks of the matrix indicates that this 50 nm Au/NaCl layer grown at  $T=400^\circ\text{C}$  is primarily an epitaxial layer with a relatively low (but clearly detectable) density of twins. As the diffraction intensity scales with the crystalline volume, the volume of twins can be estimated in the order of 0.1%. The presence of nanotwins was confirmed by a TEM observation on a plane view sample. The Bright Field micrograph on Fig. 5 clearly shows numerous {111} nanotwins regularly distributed. Their length is ranging between 20 and 80 nm and their thickness is less than 10 nm. Note that the thickness of the twins has been estimated as the size of black domains. Indeed, we assume that, due to lamellae orientation and to crystallographic considerations, the width of black domains can be assigned as twins' thickness. As in other fcc metals with a low SFE, many authors [19-21] have already observed those {111} twins in gold single crystal. {111} twins have also been reported by Miller *et al.* in polycrystalline gold thin films elaborated by electron beam evaporation on silicon [33]. Noteworthy our gold single crystal seems to have twins that have similar geometrical dimensions than the smaller ones observed by Matthews [21] while the twins

reported by Dehm *et al.* [17] and Gruber *et al.* [23] were much longer (a few microns). While out of the scope of the present paper, the presence of twins may enable an important interfacial energy dissipation mechanism and can be formed during crystal growth (growth twins). However, the twin nucleation and growth might happen during cooling from fabrication temperature to room temperature and, the thickness of a twin might change in response to an applied loading. Dehm *et al.* [17] justify the density of twins by a kinematical and thermodynamical approach. The twins would nucleate during the cooling to room temperature to relax the strain induced by the large difference of coefficient of thermal expansion between NaCl substrate and gold foil. Similar  $\{111\}$  pole figures exhibiting such secondary peaks attributed to twins have been reported on low SFE materials such as Cu [34] and Ag [35]. The latter authors attributed the nucleation of twins to the low energy of  $\{111\}$  facets at the growth front while Wang *et al.* [34] observed that the growth of twins was directly related to the flux of incident atoms. In our case, even if the gold growing condition are different from the one of Cu and Ag, the assumption based on strain relaxation proposed by Dehm *et al.* [17] seems to be not appropriate as we experienced that smaller temperatures of growth induced larger diffraction intensities of peaks related to the twins.

### **3.2 Evolution of twinned volume during in situ deformation test**

As mentioned in section 2.2, the pole figures are acquired with a XPAD 2D detector. It is worth noting that the diffraction patterns corresponding to matrix and to  $\{111\}$  twins exhibit streaks (see Fig. 2). Diffraction streaks derive from the loss of translation invariance; this phenomenon is well-known along the surface normal direction for example. In our gold film, those streaks are induced by the presence of the surface and the interface with the substrate and also by the presence of the twins. For the (111) Bragg peak related to the gold matrix, the streaks are completely negligible. But for the (111) Bragg peak related to the twin volume, this streak has an intensity as high as the diffracting volume of the twins itself because the twins are very thin.

Theoretically, the streak is perpendicular to the twin boundaries and induces an apparent variation of  $2\theta$  angle along  $\psi$  in the pattern of Fig. 2. As the intensity of the streak is of the same order as the intensity of the peak itself, it is difficult to measure precisely the  $2\theta$  position of the Bragg peak related to the twins and to extract microstructural plastic features from the shape of the peak [36]. Hence, the present study only focuses on the intensity evolution of the peak, i.e. evolution of the integrated intensity of the peaks on the pole figures. As mentioned previously, the diffraction intensities of a pole figure scale with the crystalline volume with the specific orientation associated to  $\phi$  and  $\psi$ , i.e. with the volume of twins. The integrated intensity is determined from the two-dimensional intensity distribution on the pole figure considering a large  $\phi$  and  $\psi$  ranges to determined and subtract the background ( $\phi$  range of  $32^\circ$  and  $\psi$  range of  $24^\circ$ ).

Fig. 6 shows a few pole figures that have been chosen for 4 applied true strain increments during loading, namely 0.2%, 1.1%, 2.1%, 3%, 4% and unloading 1.8%. Only a small  $\psi$  range of the recorded pole figures is shown in Fig. 6 to clearly highlight the main features that change during the deformation test. The 3 peaks at about  $\psi \sim 16^\circ$  are related to the  $\{111\}$  through-thickness twins I, II and III. The horizontal tensile axis lay near the direction  $[110]$  of gold single-crystal at an angle of about  $7^\circ$ . Defining  $[110]$  as the tensile direction, twins I and III correspond to twins with twin-boundaries parallel to  $(111)$  and  $(\bar{1}\bar{1}1)$  planes respectively and the twins II have their interfaces parallel to  $(\bar{1}11)$  planes. In other words, twins II may be described as parallel to the tensile direction. The intensity distribution corresponding to twins I and III is drastically increasing while the one corresponding to twins II is slightly decreasing. This observation is clearly shown in Fig. 7 where the integrated intensity of those peaks is plotted versus the applied true strain  $\epsilon_{11}$ . The integrated intensity is not exactly the same for twins I and III at the beginning of the tensile test, but the increase is quite similar for both

twins: the intensity is multiplied by a factor of 4 to 5 during uniaxial straining up to 4%. At the same time, the integrated intensity of the twins II peak decreases by about only 25% in the perpendicular direction. During unloading, after a small plateau at the beginning of the unloading, the integrated intensity of the twins I and III is decreasing by 35-50% while nothing significant is observed for twins II.

The curves in Fig. 7 may be interpreted in term of plastic features as the following: (i) for an applied uniaxial tensile straining, the volumes of through-thickness  $\{111\}$  twins I, II and III are constant up to an applied strain of about 1%; (ii) then, as the applied strain increases from 1% up to 4%, the volume of  $(111)$  and  $(\bar{1}\bar{1}1)$  twins is drastically increasing of about 400-500% while the volume of  $(\bar{1}11)$  twins that are parallel to the straining direction is slightly decreasing (of about 25%). In other words, the elasto-plastic behavior of the Au single-crystal foil is mainly based on slip mechanisms up to an applied uniaxial strain of 1%. The present experiment did not allow capturing the yield point, so the exact amount of plastic deformation is not known. Then, for applied uniaxial true strains from 1 up to 4%, the plastic deformation mechanism is partly based on twinning-mediated plastic deformation mode; our results cannot quantify the relative proportion of slip and twinning mechanisms. Obviously, the twinning deformation mode requires dislocation activity as slip mechanism. A review of the mechanical twinning has been provided by Christian and Mahajan [1].

As mentioned in the introduction, the fact that the single crystal of gold undergoes plastic deformation through the appearance of mechanical twin bands has already been reported a long time ago, in 1960, by Catlin and Walker [20] and, more precisely studied by Matthews ten years later [21]. The deformed gold films contained numerous very long narrow deformation twins (several microns long) with high density of small twins in between. Matthews [21] concluded that the comparison of the growth and deformation twins suggests that the deformation twins were formed by elongation of the growth twins. Although this mechanism

could be applied in the present experiment to explain the large increase of the intensity related to the twins, it is necessary to notice that the 2 deformation experiments are certainly carried out under very different deformation conditions, namely the deformation range and deformation rate. In his experiments, Matthews either cleaved the substrate with the film attached to it either glue the film to a tape that is stretched to about 1%. Much more recently, in their experiment, Oh *et al.* [22] did not report any growth of twins (or increase of twin density) in their gold single crystal during the *in situ* TEM straining. They mainly observed dislocation activity and, for a 40 nm thick gold film, they observed large partial dislocation spacings and creation of stacking fault. This visible stacking fault was erased by a second partial that was emitted at the same position. Noteworthy, the microstructure of their gold films seems to be different from the one shown in Fig. 4 of the present paper. Indeed the growth twins were very long (a few microns) in their case, and these authors did not report any density of small twins as in the present case. Only the thickness of twins is of the same order (less than 10 nm). Gruber *et al.* observed by post mortem TEM analysis that the twin density was higher after deformation, but they noted that their 40 nm thick gold single crystal contains a relatively high density of holes [23]. The observed {111} twins before and after deformation were very long compared to the one present in our sample and most of them started and ended at holes or on another twin. To compare our results with these two *in situ* experiments, independently of the difference of initial microstructure, it is also important to note that the tensile tests were performed along the [100] direction and not in the [110] as in the present paper. Obviously the deformation mechanisms are strongly dependent on the tensile direction in relation to the crystallographic direction. A tensile deformation along [110] may activate only two twinning systems contrary to the direction [100] for which the four twinning systems are equivalent. Considering the [110] direction, the two activated systems are (111)[ $\bar{1}\bar{1}2$ ] and ( $\bar{1}\bar{1}1$ )[112] with the same resolved shear and a highest Schmid factor of 0.47. It is probable that the initial

growth  $\{111\}$  nanotwins are suitable nuclei for deformation twins and the huge increase of intensity could be justified by the elongation or thickening of these initial  $\{111\}$  nanotwins. Further experimental evidence should be necessary to prove this comment. Indeed, if nanotwins may be considered as precursors for deformation twinning, the enhancement of the twin volume fraction can be dominated by the nucleation of new lamellar structures rather than by the expansion of previously existing ones as it has been reported in TWIP steels [37]. In this material, twins appear in stacks of thin, nanoscale lamellae with small thickness.

During the loading up to 4%, the Au single-crystal foil undergoes elastic and plastic deformation if we assume no crack regime. Indeed, as mentioned in section 2, the fact that the gold thin film is supported by a polymer delays the necking and cracking processes [24, 25]. Cracking happens during tensile testing for metallic thin films on polymer substrates at relatively low deformation of about 3% for Ni [38] or Cu [39]. Even if cracks may be difficult to observe, no significant crack evidence has been reported for deformation up to 15% in very ductile materials such as gold [40]. We can therefore consider that there is no cracking at tensile straining of 4% in the present experiment. The exact amount of plastic strain has not been evidenced experimentally but it is obviously between 3 to 4%. So, whatever the mechanism of dislocation-based plasticity or twinning-based plasticity, such amount of plastic deformation should induce a compressive stress state during unloading [41, 42]. Indeed the polyimide substrate which has an elastic limit much higher than the one of gold single-crystal contracts to smaller length (larger than its initial length because of a given amount of plastic deformation in the cruciform shape substrate as mentioned in the section 2.1) when the external applied load is removed from the film-substrate composite. So the gold single crystal may deform: (i) elastically at the beginning of the unloading, (ii) then plastically in compression because of the contraction of the polyimide. These 2 deformation regimes should justify the shape of the curves in Fig. 7 during unloading. The unloading part starts with a plateau as the applied true

strain decreases from 4 to approximately 3%. Then, a decrease of the intensity of the two peaks related to twins I and III that can be explained by detwinning during compressive stress state. Noteworthy the rate of detwinning during unloading as a function of applied strain is roughly similar to the one of twinning during loading. Detwinning has been experimentally observed in fcc metals. For example, Li *et al.* reported that the primary plastic deformation transits from inclined dislocation gliding to detwinning in nano-twinned polycrystalline Cu when twin thickness decreases from 25 nm to 4 nm [43]. Detwinning has also been reported during straining in a nano-polycrystalline Pd films containing a high density of twins while twinning is observed for the same materials with a lower density of twins [44]. In gold nanowires, successive tension-compression test revealed that the compressive strain was accommodated by a detwinning process [45].

#### **4. Conclusions**

We have determined some mechanical characteristic of gold single-crystal thin film supported by a polymer sample. The as-deposited gold single crystal contains small amount of {111} twins. These small through-thickness {111} twins, probably formed during film crystal growth, are about 5-10 nm thick and about 20-80 nm long. The 50 nm thick gold single crystal has been submitted at room temperature to an uniaxial deformation test in the Au [110] direction from 0% up to tensile strain of 4% and then unloaded to a tensile strain of 1.8%.

*In situ* x-ray pole figure measurements evidenced the strong evolution of the diffracting volumes related to the (111) and ( $\bar{1}\bar{1}1$ ) twins which increase of about 450% as the applied strain increases from 1 to 4%. At the same time, the diffracting volume related to the twins that are parallel to the tensile direction, i.e. ( $\bar{1}11$ ) twins, decreases of only 25%. The deformation seems to start *via* traditional crystallographic slip with no evidence of twinning before an uniaxial strain of 1%. Then x-ray pole figure measurements identify deformation twinning as

an important deformation mechanism for uniaxial strain of 1% up to 4%, however these measurements cannot capture any changes induced by slip mechanism. In other words, the plastic deformation mechanisms are partly based on twinning-mediated plastic deformation mode. The present results can quantify precisely the relative increase of twinning volume but not the relative amount of slip and twinning mechanisms for applied uniaxial true strains from 1 up to 4%.

During unloading, i.e. uniaxial reverse straining from 4% down to 1.8%, x-ray pole figure measurements evidenced also a significant evolution of the diffracting volumes related to the (111) and ( $\bar{1}\bar{1}1$ ) twins which decrease of about 40%. Concomitantly the diffracting volume related to the twins that lie in the parallel direction to the tensile direction, i.e. ( $\bar{1}11$ ) twins, did not evolve within the experimental uncertainty. The decrease of intensity is attributed to a decrease of diffracting volume related to the (111) and ( $\bar{1}\bar{1}1$ ) twins, i.e. to a detwinning process. This detwinning happens during unloading if we consider the whole sample, i.e. the composite gold/polyimide; but it is in fact a reverse loading for the gold single crystal. In other words, the detwinning happens at small applied compressive strains in the gold single-crystal film; it is due to reversible compression in the same direction. As the twinning process the detwinning affects only the two twin variants, i.e. (111) and ( $\bar{1}\bar{1}1$ ) twins. The ( $\bar{1}11$ ) twins that lie in the parallel direction to the tensile direction are not affected by the deformation test. This work demonstrates the interest of x-ray texture analysis by proving the existence of deformation twinning, by quantifying the relative evolution of the twin volume for the [110] tensile or compressive directions.

## **Acknowledgements**

This work partially pertains to the French Government program “investissements d’avenir” (LABEX INTERACTIFS, reference ANR-11-LABX-0017-01) and has been partially supported by “Nouvelle Aquitaine” Region and by European Structural and Investment Funds (ERDF reference: P-2016-BAFE-94/95). Synchrotron SOLEIL is acknowledged for allocated beamtime.

List of references:

- [1] J. W. Christian, S. Mahajan “Deformation twinning” *Prog. Mater. Sci.*, 39 (1–2) (1995), pp. 1-157
- [2] L. Remy “The Interaction Between Slip and Twinning Systems and the Influence of Twinning on the Mechanical Behavior of FCC Metals and Alloys”. *Met. Trans. A* 12 (1981) 387-408.
- [3] X. Zhang, A. Misra, H.Wanga, T.D. Shen, M. Nastasi, T.E. Mitchell, J.P.Hirth, R.G.Hoagland, J.D.Embury,” Enhanced hardening in Cu/330 stainless steel multilayers by nanoscale twinning” *Acta Mater.* 52 (2004) 995-1002
- [4] L. Lu, Y. Shen, X. Chen, L. Qian, K. Lu, “Ultrahigh strength and high electrical conductivity in copper”, *Science*, 304 (2004) 422-426
- [5] L. Lu, R. Schwaiger, Z.W. Shan, M. Dao, K. Lu, S. Suresh, “Nano-sized twins induce high rate sensitivity of flow stress in pure copper”*Acta Mater.* 53 (2005) 2169-2179
- [6] F. Sansoz, H.C. Huang, D.H. Warner, “An atomistic perspective on twinning phenomena in nano-enhanced fcc metals” *JOM* 60 (2008) 79-84

- [7] Y. T. Zhu, X.Z. Liao, X.L. Wu, “Deformation twinning in nanocrystalline materials” *Prog. Mater. Sci.* 57 (2012) 1-62
- [8] Twinning in metallic materials, *MRS Bulletin*, volume 41 (2016)
- [9] Q. Yu, Z.W. Shan, J. Li, X. Huang, L. Xiao, J. Sun and E. Ma, “Strong crystal size effect on deformation twinning” *Nature*, 463 (2010) 335-338
- [10] H.S. Park, K. Gall, J.A. Zimmermann, “Deformation of fcc nanowires by twinning and slip” *J. Mech. Phys. Solids* 54 (2006) 1862–1881
- [11] R. Bejaud, J. Durinck and S. Brochard “The effect of surface step and twin boundary on deformation twinning in nanoscale metallic systems” *Computational Mater. Science* 145 (2018) 116-125
- [12] J. Ye, R.K. Mishra, A.K. Sachdev and A.M. Minor “In situ TEM compression testing of Mg and Mg–0.2 wt.%Ce single-crystals” *Scripta Mater.* 64 (2011) 292–295
- [13] S. Ino, D. Watanabe, S. Ogawa “Epitaxial growth of metals on rocksalt faces cleaved in vacuum. I” *J. Phys. Soc. Jpn.* 19 (1964) 881– 891
- [14] S. Ino “Epitaxial Growth of Metals on Rocksalt Faces Cleaved in Vacuum. II. Orientation and Structure of Gold Particles Formed in Ultrahigh Vacuum” *J. Phys. Soc. Jpn.* 21 (1966) 346– 362
- [15] J.W. Matthews “Growth of Face-Centered-Cubic Metals on Sodium Chloride Substrates”, *J. Vac. Sci. Technol.* 3 (1966) 133–145
- [16] J. W. Matthews, D.L. Allinson “Influence of substrate steps on arrangement of defects in evaporated films” *Philos. Mag.* 8 (1963) 1283– 1303

- [17] G. Dehm, S.H. Oh, P. Gruber, M. Legros, F.D. Fischer “Strain compensation by twinning in Au thin films: experiment and model” *Acta Mater.* 55 (2007) 6659-6665
- [18] B. Wang, H. Idrissi, M. Galceran, M.S. Colla, S. Turner, S. Hui, J.P. Raskin, T. Pardoen, S. Godet, D. Schryvers “Advanced TEM investigation of the plasticity mechanisms in nanocrystalline freestanding palladium films with nanoscale twins” *Intern. J. Plast.* 37 (2012) 140-156
- [19] M.W. Chen, E. Ma, K.J. Hemker, H.W. Sheng, Y.M. Wang, X.M. Cheng “Deformation twinning in nanocrystalline aluminum” *Science* 300 (2003) 1275-1277
- [20] A. Catlin and W.P. Walker “Mechanical properties of thin single-crystal gold films” *J. Appl. Phys.* 31 (1960) 2135-2139
- [21] J.W. Matthews “Role of deformation twins in the fracture of single-crystal films” *Acta Metallurgica* 18 (1970) 175-181
- [22] S.H. Oh, M. Legros, D. Kiener, P. Gruber, G. Dehm “In situ TEM straining of single crystal Au films on polyimide: change of deformation mechanisms at the nanoscale” *Acta Mater.* 55 (2007) 5558-5571
- [23] P.A. Gruber, C. Solenthaler, E. Arzt, R. Spolenak “Strong single-crystalline Au films tested by a new synchrotron technique” *Acta Mater.* 56 (2008) 1876–1889
- [24] S.P. Lacour, S. Wagner, Z. Huang and Z. Suo “Stretchable gold conductors on elastomeric substrates” *Appl. Phys. Lett.* 82 (2003) 2404-2046
- [25] T. Li, Z.Y. Huang, Z.C. Xi, S.P. Lacour, S. Wagner and Z. Suo “Delocalizing strain in a thin metal film on a polymer substrate” *Mechanics of Materials* 37 (2005) 261–273

- [26] G. Geandier, D. Thiaudière, R.N. Randriamazaoro, R. Chiron, S. Djaziri, B. Lamongie, Y. Diot, E. Le Bourhis, P.O. Renault, Ph. Goudeau, A. Bouaffad, O. Castelnau, D. Faurie, F. Hild, “Development of a synchrotron biaxial tensile device for in situ characterization of thin films mechanical response” *Rev. Sci. Instrum.*, 81 (2010) 103903(1)-103903(8)
- [27] R.M. Langford and C. Clinton “In situ lift-out using a FIB-SEM system” *Micron* 35 (2004) 607-611
- [28] G. Besnard, F. Hild, S. Roux, ““Finite-Element” Displacement Fields Analysis from Digital Images: Application to Portevin–Le Châtelier Bands” *Exp. Mech.*, 46 (2006) 789-803
- [29] S. Djaziri, P.O. Renault, F. Hild, E. Le Bourhis, P. Goudeau, D. Thiaudière and D. Faurie, “Combined synchrotron X-ray and image-correlation analyses of biaxially deformed W/Cu nanocomposite thin films on Kapton” *J. Appl. Cryst.* 44 (2011) 1071-1079.
- [30] P. Pangaud, S. Basolo, N. Boudet, J.-F. Berar, B. Chantepie, J.-C. Clemens, P. Delpierre, B. Dinkespiler, K. Medjoubi, S. Hustache, M.Menounia, C. Morel “XPAD3-S: A fast hybrid pixel readout chip for X-ray synchrotron facilities,” *Nucl. Instrum. Methods Phys. Res., Sect. A* 591 (2008) 159–162.
- [31] C. Mocuta, M.-I. Richard, J. Fouet, S. Stanescu, A. Barbier, C. Guichet, O. Thomas, S. Hustache, A. V. Zozulya and D. Thiaudiere, “Fast pole figure acquisition using area detectors at the DiffAbs beamline – Synchrotron SOLEIL” *J. Appl. Cryst.* 46 (2013) 1842–1853.
- [32] P. Godard, P.O. Renault, D. Faurie, D. Thiaudière “Relaxation Mechanisms in a Gold Thin Film on a Compliant Substrate as Revealed by X-Ray Diffraction” *Appl. Phys. Lett.* 110 (2017) 211901

- [33] D.C. Miller, C.F. Herrmann, H.J. Maier, S.M. George, C.R. Stoldt, K. Gall, “Thermo-mechanical evolution of multilayer thin films: Part II. Microstructure evolution in Au/Cr/Si microcantilevers” *Thin Solid Films* 515 (2007) 3224–3240.
- [34] P. Wang, H. Li, T.M. Lu, “Orientation modulated epitaxy of Cu nanorods on Si(001) substrate” *IEEE Trans. On Nanotech.* 11 (2012) 542-545.
- [35] J.S. Chawla and D. Gall “Epitaxial Ag(001) grown on MgO(001) and TiN(001): twinning, surface morphology, and electron surface scattering” *J. Appl. Phys.* 111 (2012) 043708.
- [36] Z. Budrovic, H. Van Swygenhoven, P.M. Derlet, S. Van Petegem, B. Schmitt, “Plastic deformation with reversible peak broadening in nanocrystalline nickel” *Science* 304 (2004) 273-276.
- [37] D.R. Steinmetz, T. Jäpel, B. Wietbrock, P. Eisenlohr, I. Gutierrez-Urrutia, A. Saeed-Akbari, T. Hickel, F. Roters, D. Raabe, “Revealing the Strain-Hardening Behavior of Twinning-Induced Plasticity Steels: Theory, Simulations, Experiments.” *Acta Mater.* 61 (2013) 494–510.
- [38] D. Faurie, F. Zighem, P. Godard, G. Parry, T. Sadat, D. Thiaudiere, P.-O. Renault “In situ x-ray diffraction analysis of 2D crack patterning in thin films” *Acta Mater.* 165 (2019) 177-182
- [39] M.J. Cordill, V.M. Marx “Fragmentation testing for ductile thin films on polymer substrates” *Phil. Mag. Lett.* 93 (2013) 618-624.

- [40] B. Putz, R.L. Schoeppner, O. Glushko, D.F. Bahr and M.J. Cordill “Improved electro-mechanical performance of gold films on polyimide without adhesion layers” *Scripta Materialia* 102 (2015) 23–26
- [41] M. Hommel, O. Kraft, and E. Arzt, A new method to study cyclic deformation of thin films in tension and compression, *J. Mater. Res.* 6 (1999) 2373-2376
- [42] P.O.Renault, P.Villain, C.Coupeau, P.Goudeau, K.F.Badawi “Damage mode tensile testing of thin gold films on polyimide substrates by X-ray diffraction and atomic force microscopy” *Thin Solid Films* 424 (2003) 267-273
- [43] X. Li, Y. Wei, L. Lu, K. Lu, H. Gao “Dislocation nucleation governed softening and maximum strength in nano-twinned metals” *Nature* 464 (2010) 877–880
- [44] A. Kobler, J. Lohmiller, J. Schäfer, M. Kerber, A. Castrup A. Kashiwar, P.A. Gruber, K. Albe, H. Hahn and C. Kübel “Deformation-induced grain growth and twinning in nanocrystalline palladium thin films” *Beilstein J. Nanotechnol* 4 (2013) 554–566
- [45] S. Lee, J. Im, Y. Yoo, E. Bitzek, D. Kiener, G. Richter, B. Kim, S.H. Oh “Reversible cyclic deformation mechanism of gold nanowires by twinning-detwinning transition evidenced from in situ TEM” *Nat. Commun.* 5 (2014) 3033.

## List of figure captions

Figure 1: Schematic of experimental set-up for the definition of diffraction angles, namely  $\psi$  inclination angle of diffraction planes relatively to the normal surface,  $\phi$  the azimuthal angle and  $2\theta$  the Bragg angle. On the left, typical pattern recorded with the 2D detector XPAD.

Figure 2: On the left: as-recorded typical diffraction pattern recording with the XPAD 2D detector in the diffracting condition corresponding to the  $\{111\}$  planes belonging to the twins. On the right: corresponding 2D diffraction pattern recalculated in the angular space  $(2\theta, \psi)$ . Noteworthy the distribution of intensity corresponding to gold is not constant as a function of  $2\theta$  as underlined by the dashed line. In other word, the 2D pattern exhibits a streak. As the twins are very thin, this streak has intensity as high as the diffracting volume of the twins itself and, theoretically, it is perpendicular to the twin boundaries.

Figure 3: True strains ( $\epsilon_{11}$ ,  $\epsilon_{22}$ ) measured by DIC at the center of the cruciform shape substrate versus number of images. The corresponding applied loads are given for the two arms of the substrate. The inset shows the strain relaxation that happens for the larger loads only: a decrease of about 0.1% during x-ray collection time for an applied true strain of about 3.8%.

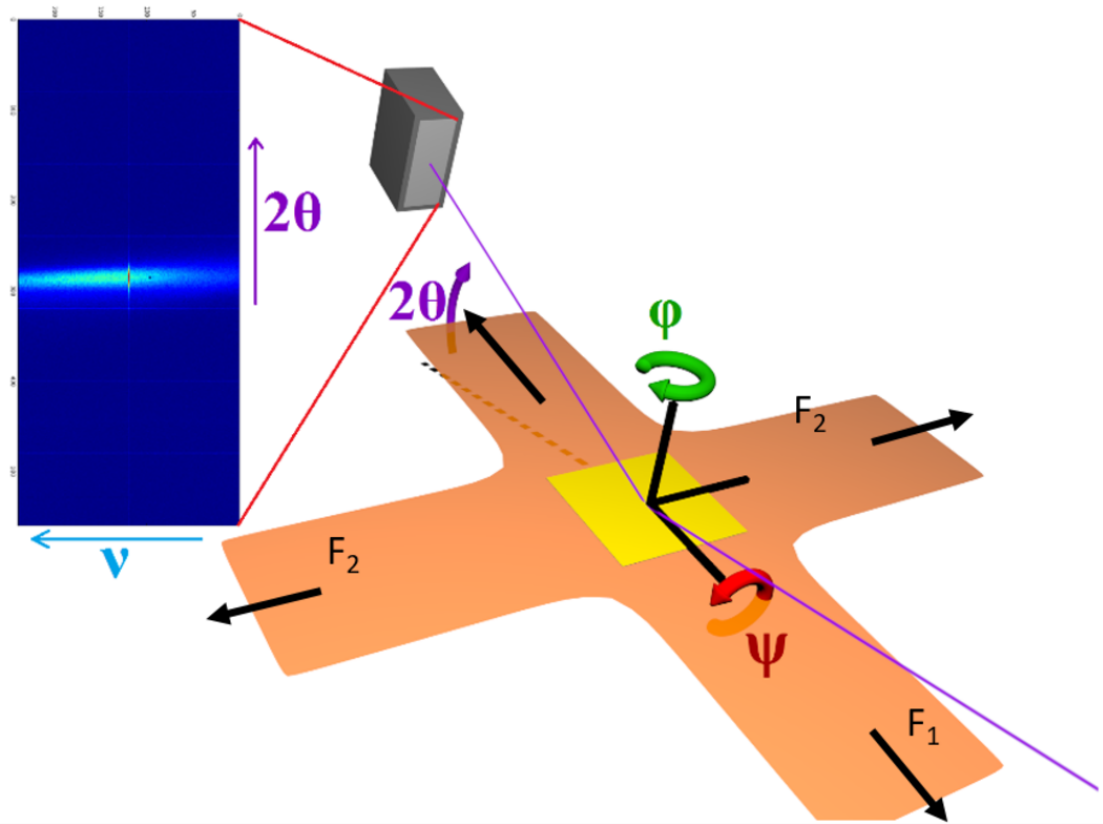
Figure 4: X-ray pole figure constructed from the (111) diffraction peak of the sample grown at  $T = 400\text{ }^\circ\text{C}$  on NaCl. The four-fold symmetry in  $\{111\}$  poles indicates that the sample is [001] oriented. The direction [100] of NaCl is indicated to show the cube on cube growth. The four

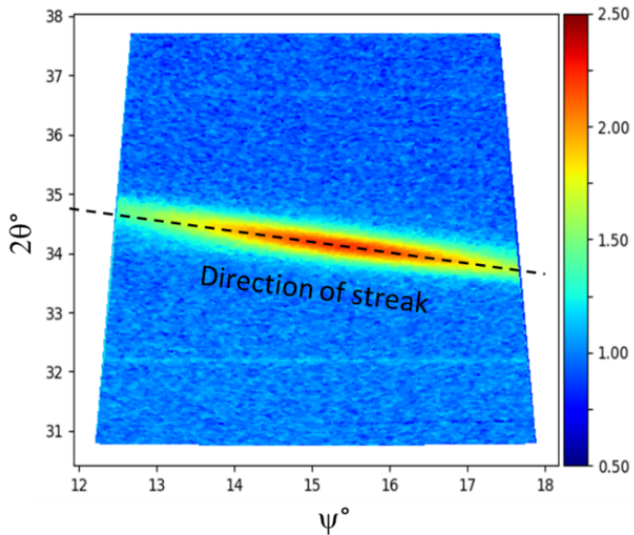
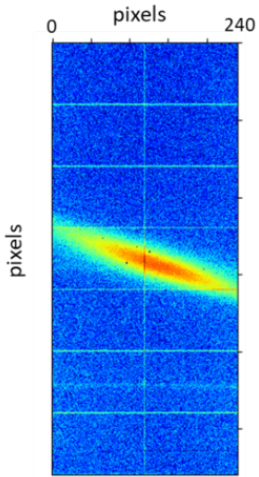
main peaks are induced by the gold single-crystal. The secondary peaks correspond to the four  $\{111\}$  twin variants. As for example, the peaks induced by twins I, i.e. (111) twins, are indicated by the dotted circles at inclinations  $\psi$  of  $16^\circ$ ,  $55^\circ$  and  $79^\circ$ . At  $55^\circ$ , the peak is overlapped by the matrix.

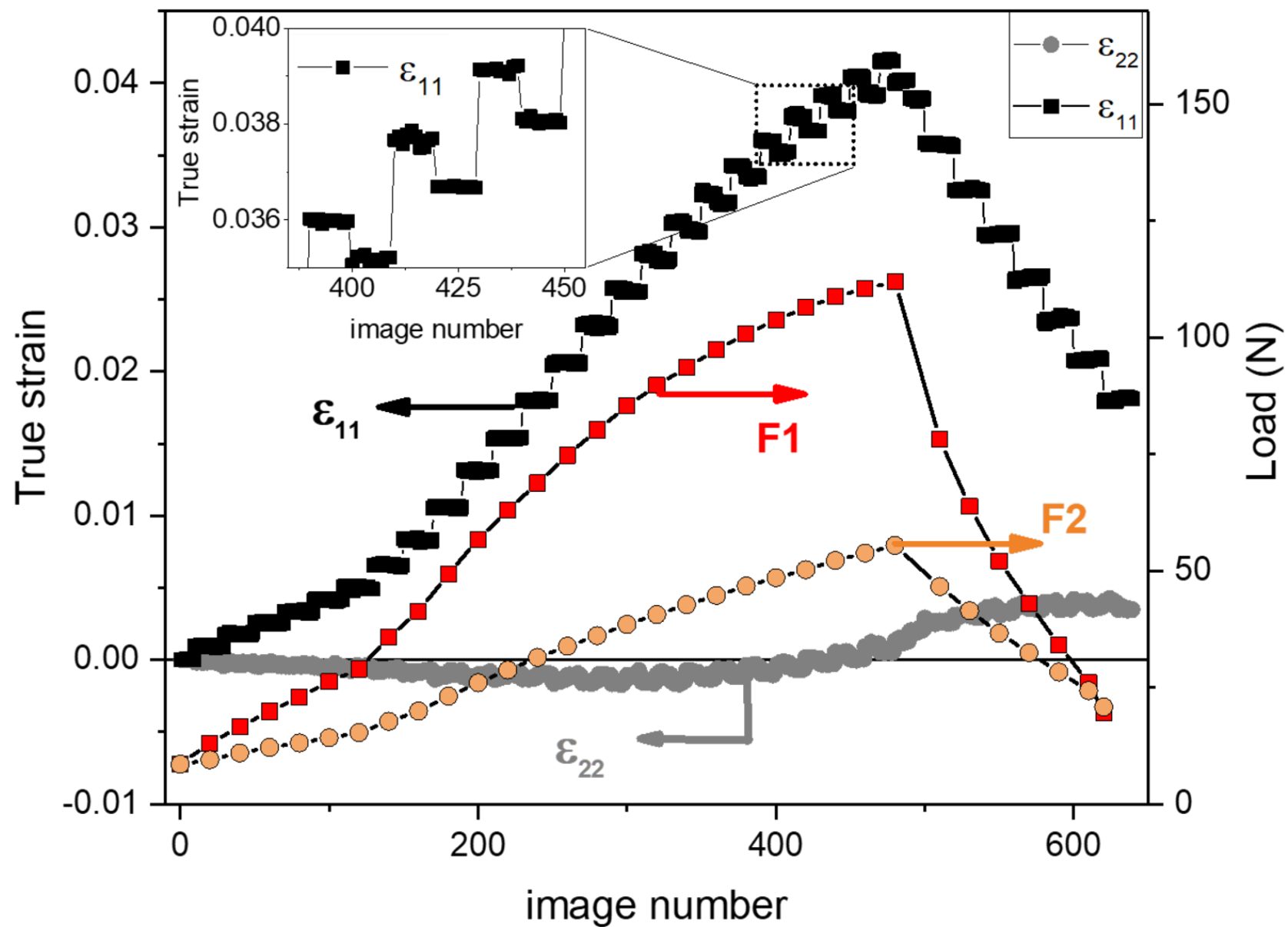
Figure 5: Top: Bright field TEM micrograph of a 50 nm thick Au single-crystal. General view showing numerous small twins of about 20-80 nm long, a few dislocations can also be observed. Bottom: General view of the gold film obtained by BF- STEM showing the twins along the [110] viewing direction, the (111) twins have a thickness of about 5-10 nm. The insets are the corresponding diffraction patterns showing the crystallographic orientation.

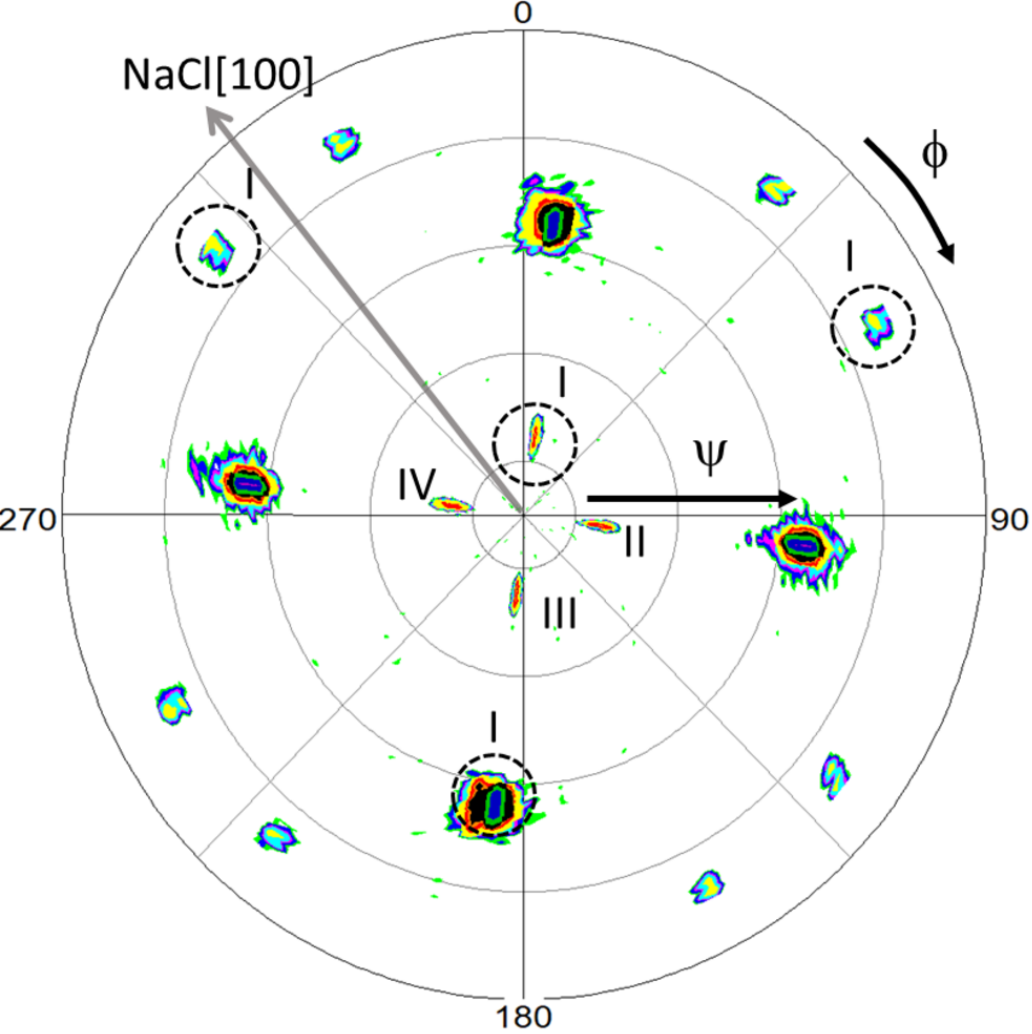
Figure 6: Selection of x-ray  $\{111\}$  pole figures acquired during uniaxial deformation test. Only the part of the pole figure that evolves during the test is shown. The true strain  $\epsilon_{11}$  whose value is indicated on each pole figure is applied horizontally (as indicated by the arrows). Note that the horizontal tensile axis lays near the direction [110] of gold at an angle of about  $7^\circ$ . The last value of 1.8% is during unloading of the gold/polyimide composite; the gold is submitted to a reverse loading in this case.

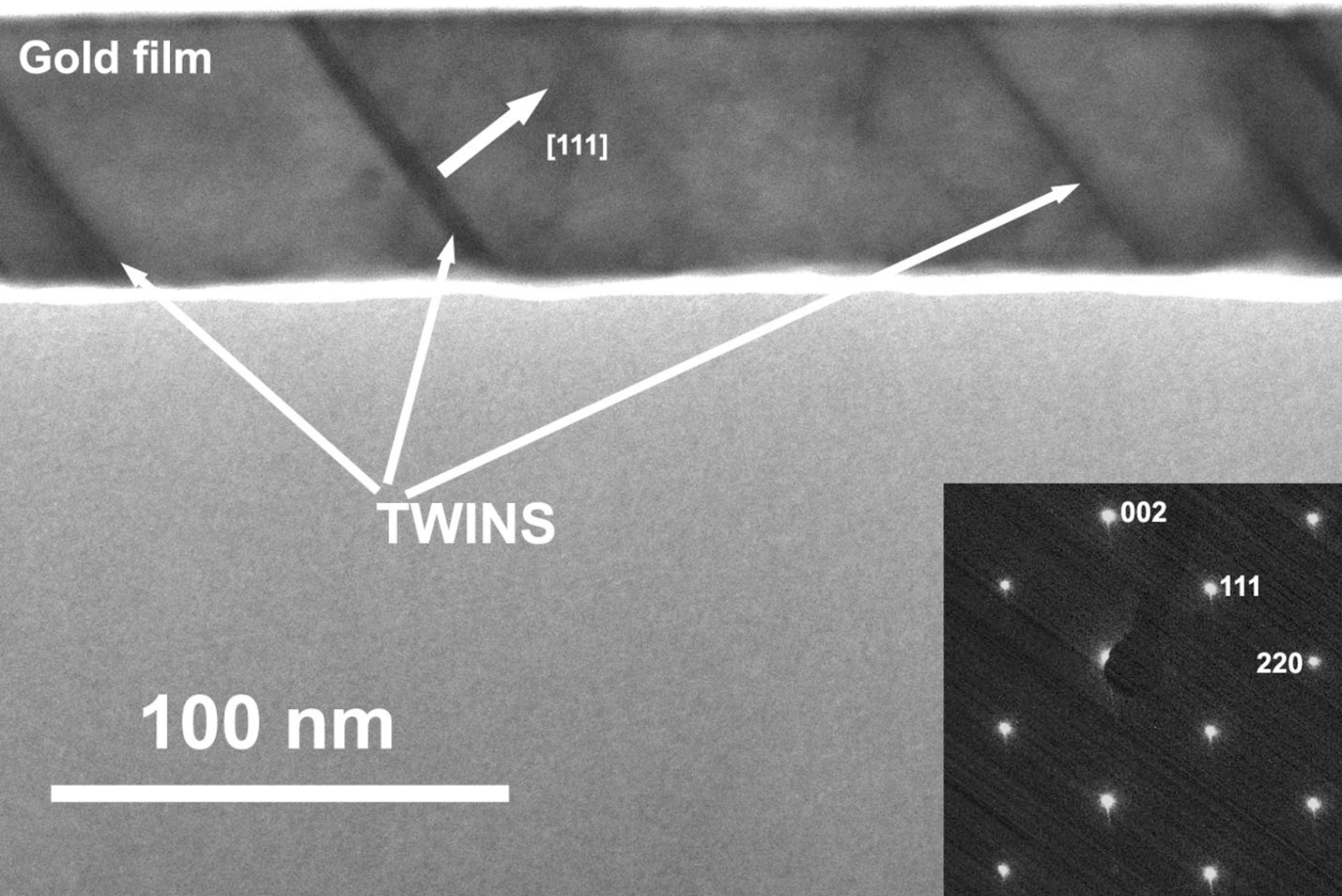
Figure 7: Integrated intensity of the secondary peaks at  $\psi \sim 16^\circ$  related to  $\{111\}$  twins versus the true strain  $\epsilon_{11}$ . Defining [110] as the tensile direction, twins I and III correspond to (111) and  $(\bar{1}\bar{1}1)$  twins respectively while twins II have their twin-boundaries parallel to  $(\bar{1}\bar{1}1)$ . In other words, twins II may be described as parallel to the tensile direction.



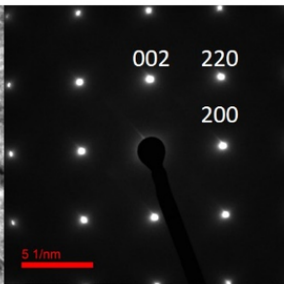








a)



500 nm

A red horizontal scale bar is located at the bottom left of the main image, with the text '500 nm' written above it.

